EE599 Magnetic Resonance Imaging and Reconstruction
Final Project Report
Jungwoo Lee (610-21-4670)

Reference : An Improved Gridding Method for Spiral MRI Using Nonuniform Fast Fourier Transform

Authors: Liewei Sha, Hua Guo, and Allen W.Song

Introduction

The objective of this project is to develop improved reconstruction algorithm using non-uniform fast Fourier transform(NUFFT) for spiral MRI. In conventional gridding methods, while explicit forms of kernel functions were used, in this paper optimized kernels are suggested minimizing reconstruction error in the least square sense between real and reconstructed images. To accomplish its goal well-known techniques such as Kaiser-Bessel gridding(KB)[3] and a generalized fast Fourier transform(GFFT)[4] are being used to put an emphasis on the new NUFFT method called LS_NUFFT[1,2] compared to conventional ones. With phantom image(128x128) provided in the homework set, the concept of improved NUFFT method and the corresponding results are presented and the difference between LS_NUFFT and previous algorithms including KB and GFFT is discussed. In order to be able to succeed in getting good reconstruction, results with different values of parameters are shown for justification. Finally, some possible modification of LS_NUFFT method is addressed in final remarks.

Method

A. Simple gridding reconstruction

Instead of using simple 2DFFT for image reconstruction, density pre-compensation function was used to reduce the low spatial artifacts caused by oversampling k-space near the origin. The analytical formula for direct summation is

$$I(x,y) = \sum_{p=1}^{M} s_p \exp(i2\pi(xk_{xp} + yk_{yp})) \qquad \text{Eq.(1)}$$

where s_p is k-space data multiplied by density pre-compensation function and p is the number of samples in spiral trajectory. kx_p and ky_p ranges over –N/2 to N/2, respectively. x and y are in [–N/2:N/2-1]/N. Here N is 128. The density compensation function and 6 interleaved spiral trajectories are shown in Fig.1. As shown in Fig.2, the resultant image has less aliasing artifact than that of homework #6 even without using a 2X grid. Due to the corrected density, suppression of low frequency artifacts is also clearly seen.

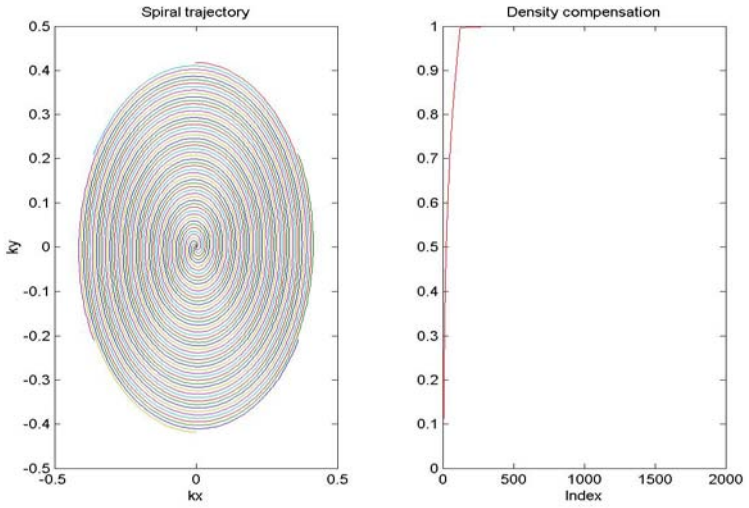

Fig.1. k-space trajectory and density compensation function

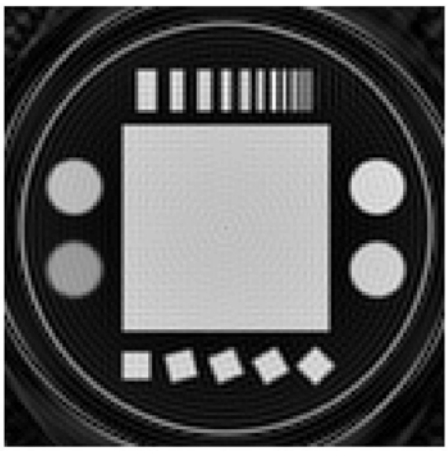

Fig.2. Reconstructed image(128x128) using direct summation

B. LS_NUFFT reconstruction

Improved NUFFT algorithm[1] named as LS_NUFFT generates kernel matrices in x-y directions to minimize the approximation error in the least square sense. After convolution of the weighted k-space data and the kernel matrices, 2DFFT on data set is performed to correct aliasing and low frequency artifacts. For further correction deapodization procedure is also taken. Kernel functions are defined as follows.

$$
\begin{aligned}
&\rho_{j,cp} = G_{j,k} a_{k,cp} \\
&G = F^{-1}, F_{j,k} = \frac{-2i\sin(\pi(j-k)/m)}{1-\exp(i2\pi(j-k)/mN)} \\
&a_{k,cp} = i\sum_{\gamma=-1,1} \frac{\sin[(\frac{\pi}{2m}(2k-\gamma-2\{mc_p\})]}{1-\exp(i\frac{\pi}{Nm}(2\{mc_p\}-2k+\gamma))} \\
&\{mc_p\} = mc_p - [mc_p] \\
&j,k = -\frac{q}{2}\cdots\frac{q}{2} \\
&p = 1,\ldots M
\end{aligned}
\qquad \text{Eq.(2)}
$$

For analytical comparison q and m set to be 2 and 3, respectively. m and q determine the field of view in reconstructed images and the resolution of inverse FFT procedure in frequency domain, respectively. M is the number of samples in spiral trajectory. Since kernel functions are separable they are independently multiplied to k-space data s_p. As mentioned before the important difference between LS_NUFFT and conventional methods is the kernel function ρ and scale factor s_c. The latter has shift invariant kernels whereas the former has shift variant ones. Because of more degree of freedom in kernels the former is more accurate than the latter. On the other hand, conventional methods are easier to implement than LS_NUFFT. The expression for LS_NUFFT reconstruction is given as follows.

$$I(x,y) = (s_c(x)s_c(y))^{-1} \sum_{p=1}^{M} s_p \sum_{j1=-q/2}^{q/2} \sum_{j2=-q/2}^{q/2} \rho_1(j1, kx_p)\rho_2(j2, ky_p) \times \exp(i2\pi(x([mk_{xp}]+j1)+y([mk_{yp}]+j2))/m) \quad \text{Eq.(3)}$$

To justify appropriate parameters for m and q, their variations over several values were tested and results are illustrated in Fig.3.

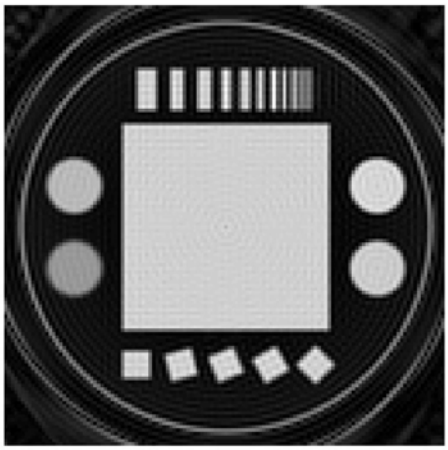

(a) LS NUFFT(m=3, q=2)

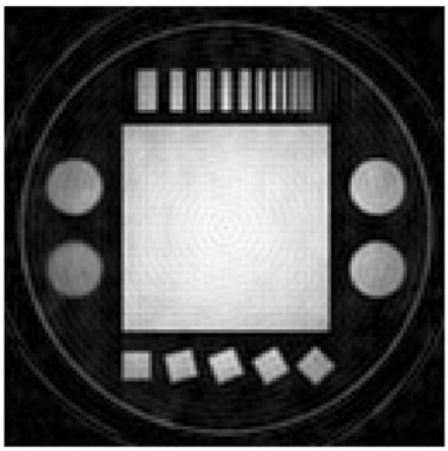

(b) LS NUFFT(m=3, q=4)

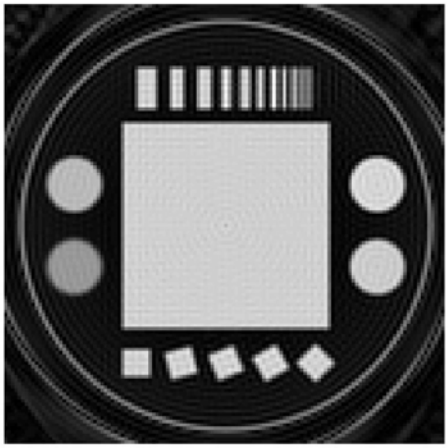

(c) LS NUFFT(m=3, q=6)

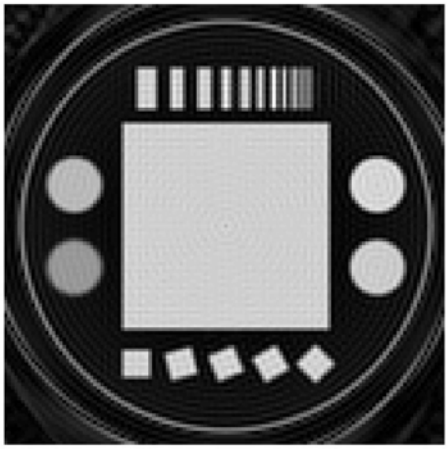

(d) LS NUFFT(m=3, q=8)

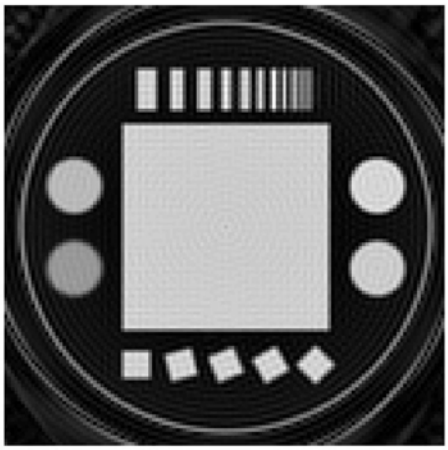

(e) LS NUFFT(m=3.5, q=2)

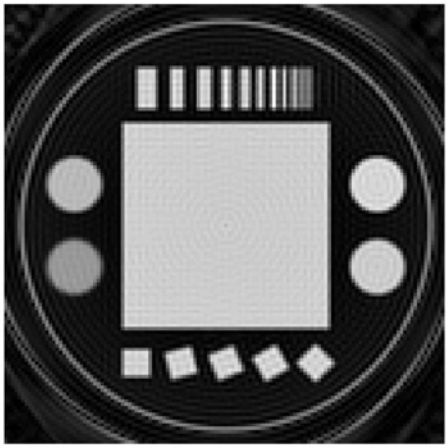

(f) LS NUFFT(m=3.5, q=4)

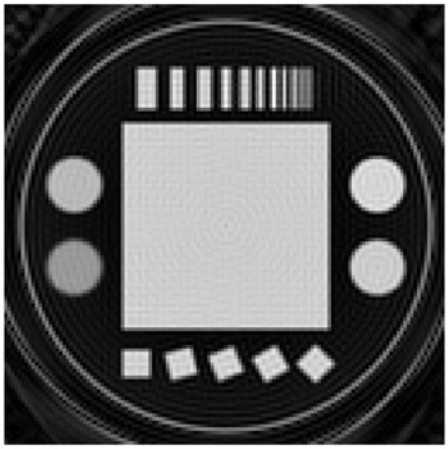

(g) LS NUFFT(m=3.5, q=6)

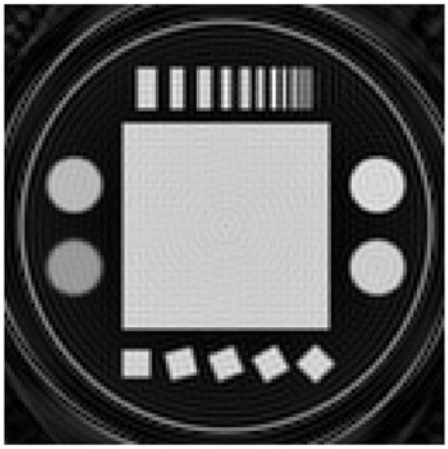

(h) LS NUFFT(m=3.5, q=8)

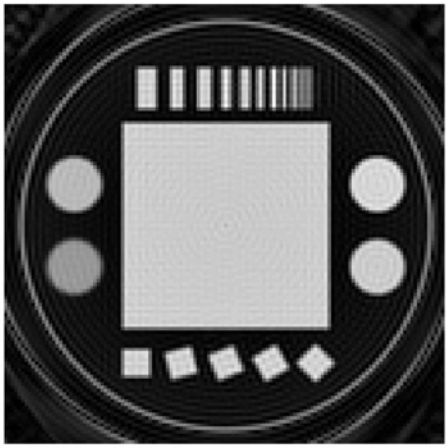

(i) LS NUFFT(m=3.8, q=2)

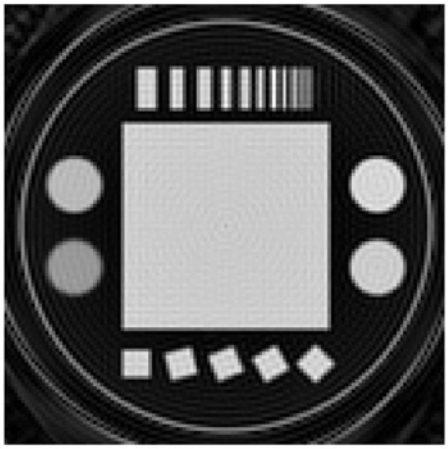

(j) LS NUFFT(m=3.8, q=4)

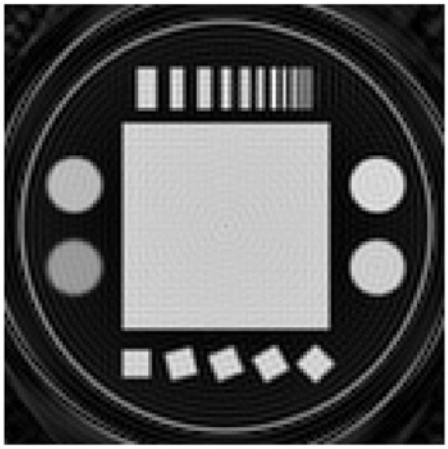

(k) LS NUFFT(m=3.8, q=6)

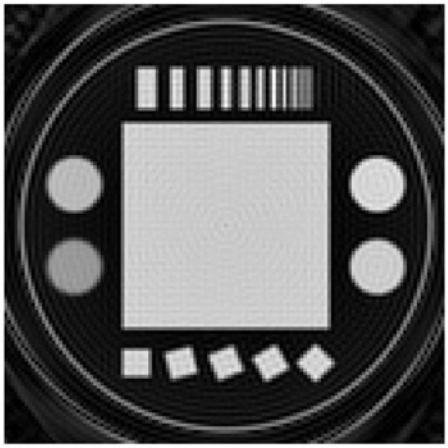

(l) LS NUFFT(m=3.8, q=8)

Fig.3. Reconstructed results corresponding to different values of m and q

Based on the distance measure(D) defined in next section, the best values for m and q were decided. Table 1 summarizes the distance measures with all cases. As shown in Table 1, it is better to have lower values of both of them. As a result m and q set to be 3 and 2, respectively. If m is less than 3 or larger than 4, however, reconstructed image depicted in Fig.4 is very poor even compared to those of conventional methods. More detail is mentioned in discussion section.

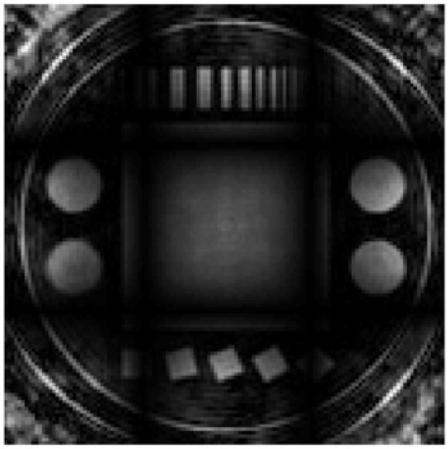

Fig.4. Reconstructed image using LS NUFFT with m=4

Table 1. Distance measures with different combination of m and q

Distance measure($Dx10^{-2}$)	q=2	q=4	q=6	q=8
m=3	2.66	7.99	15.99	238.57
m=3.5	2.69	8.08	16.17	26.95
m=3.8	2.70	8.12	16.24	27.07

C. Conventional algorithms

The most dominant difference between LS_NUFFT and conventional algorithms such as Kaiser-Bessel and generalized FFT methods lies in the fact that the former optimizes scale factor and kernel matrix in the least square sense while the latter has fixed forms of functions. In Kaiser-Bessel method, Sinc and the modified first order Bessel functions were used as scale factor and kernel matrix, respectively. For generalized FFT both of them have Gaussian functions. Those scale factors and kernel matrices are recapitulated in Table 2. To realize those algorithms in MATLAB all it takes is to replace those of LS_NUFFT with explicit functions defined in Table 2. Because of that, implementation is much easier and more straightforward than LS_NUFFT.

Table 2. Scale factors and kernel matrices for KB, GFFT and LS_NUFFT

	Kaiser-Bessel	Generalized FFT	LS_NUFFT
Scale Factor sc(x)	$\frac{\sin(\sqrt{f(x)})}{\sqrt{f(x)}}$	$\exp(-b(\frac{2\pi x^2}{m})^2)$	$\cos(\pi x / mN)$
Kernel matrix ρ(j,k)	$\frac{I_0(\beta\sqrt{1-(2(\{mk\}-j)/mq)^2})}{q}$	$\exp(-\frac{(\{mk\}-j)^2}{4b})$	$G_{j,k}a_{k,kp}$

Results

Reconstructed images based on Kaiser-Bessel, Generalized FFT, and LS NUFFT methods were presented below. The quality of reconstructions(I_r) for size of NxN is evaluated in terms of the distance measure defined as

$$D(I_r) = \frac{\|I_d - I_r\|}{N^2 \max(I_d)} \qquad \text{Eq.(4)}$$

where I_r and I_d represent reconstructed images obtained through direct summation and other methods, respectively. The result from direct summation was chosen as a standard

image for comparison with others and calculated through multiplication by conjugate phase terms at corresponding positions. Each method employs the same 6 interleaved spiral trajectories and density compensation function as already presented in Fig.1. Reconstruction results from Kaiser-Bessel and generalized FFT models are illustrated in Fig.5 and 6, respectively. In addition, distribution of values for kernel functions corresponding to conventional methods is demonstrated in Fig.7 and 8.

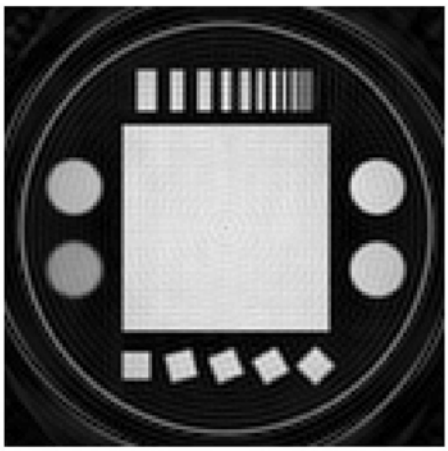

Fig.5. Reconstructed image using Kaiser-Bessel model with beta=30.544

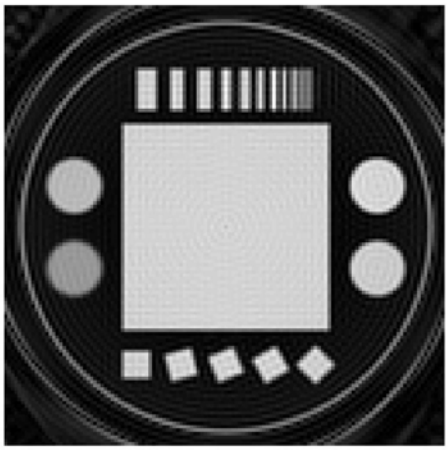

Fig.6. Reconstructed image using generalized FFT model with m=2 and b=0.1

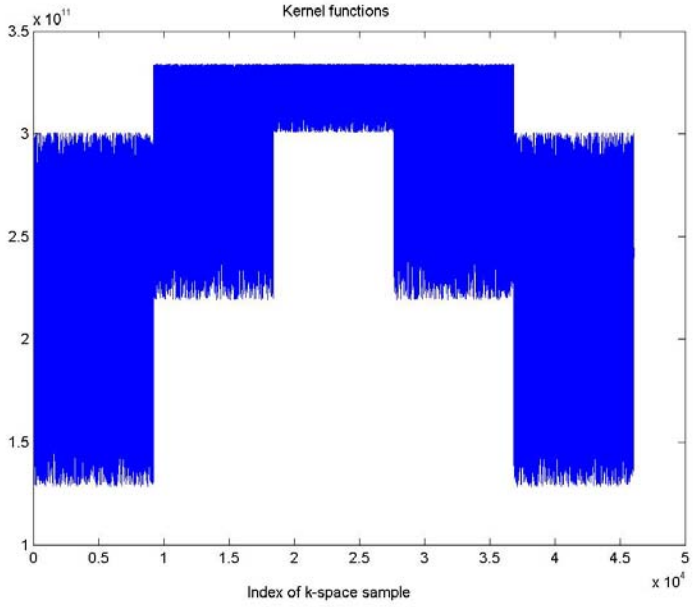

Fig.7. Kernel matrices for Kaiser-Bessel model with beta=30.544

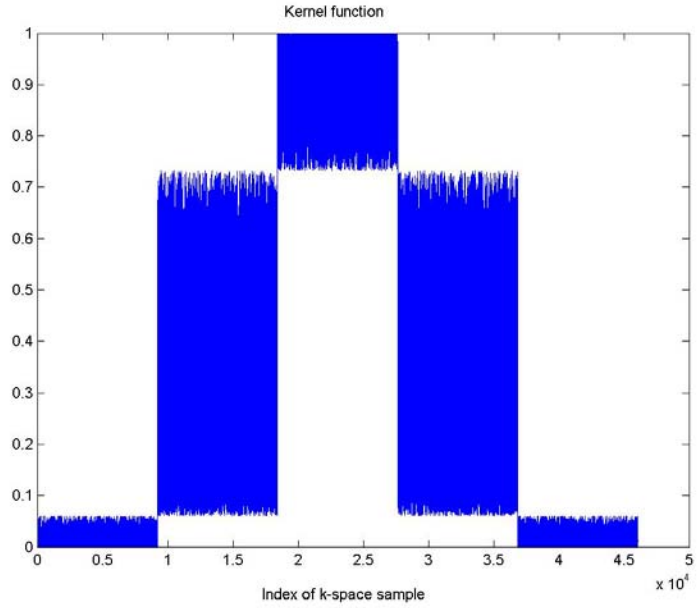

Fig.8. Kernel matrices for generalized FFT model with m=2 and b=0.1

Compared to resultant image from direct summation, it is obvious that some swirling artifact outside the object in the image of direct summation is pretty much suppressed in both conventional algorithms. Without employing 2X grid reconstruction there is little aliasing effect observed. In above results, several parameters such as β, m, and b were chosen according to the instruction in the reference[1]. Although these methods are really

dependent on parameters as well as objects to be reconstructed, decent results were obtained without any serious complication. Next, kernel matrices and resultant image computed by LS_NUFFT are shown in Fig.9 and 10, respectively.

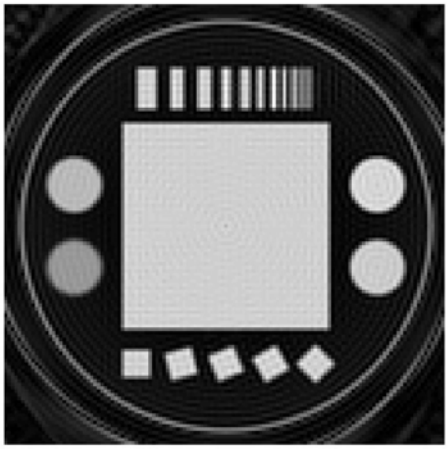

Fig.9. Reconstructed image using LS_NUFFT method with m=3 and q=2

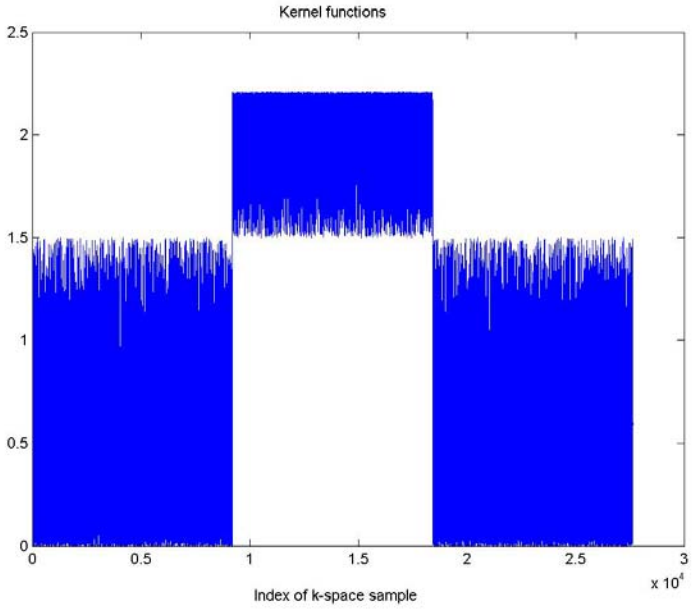

Fig.10. Kernel matrices for LS_NUFFT method with m=3 and q=2

Table 3. Distance measures for different methods such as KB, GFFT, and LS_NUFFT

	Distance measure($Dx10^{-2}$)
KB	5.83
GFFT	0.48
LS_NUFFT	2.66

It is difficult to visually decide which one performs better among three methods. For further comparison, the distance measures defined by Eq.(4) for Kaiser-Bessel(KB), GFFT, and LS_NUFFT were calculated as summarized in Table 3. As a result, GFFT is even better than LS_NUFFT. The reason for this unexpected result is discussed more in detail in following section.

Discussion

The results derived above indicate that reconstructed images using both conventional methods and LS_NUFFT have better image quality than that from direct summation in terms of low frequency artifacts, aliasing effect, and image contrast. In the reference proposed method known as LS_NUFFT is supposed to be superior to other conventional techniques including Kaiser-Bessel(KB) and generalized FFT(GFFT) methods. Unfortunately, through the simulation, different conclusion from what we had expected was drawn that GFFT has better performance even compared to LS_FFT in terms of the distance measure D. The first reason that can be ascribed to is the possibility of improper choice of kernel matrices for LS_NUFFT. Although exactly following the same way to generate kernel matrices as what was introduced in the reference material, we can see the different form of kernel distribution through the entire k-space sample.(Compare Fig.8 with Fig.10) In other words, the distribution for GFFT in Fig.8 is more similar to what was illustrated in the reference for LS_NUFFT. If the distribution of kernel matrices for LS_NUFFT is more like the one in Fig.8, then the result may be improved such that LS_NUFFT shows better quality than GFFT. The second reason is the possibility of improper parameter justification of m for LS_NUFFT. Since a limited time was allowed for this project, the reconstruction was not executed for further lower values of m. As you can tell in Table 1, the smaller m has less distance measure D which means better image quality for smaller q. Hence if it's feasible to try much smaller values of m, then more

improved image may be reconstructed by LS_NUFFT. The third reason is the improper phantom image used for the project. As already mentioned before, conventional methods have strong dependency on image quality to be reconstructed. Because the phantom applied to LS_NUFFT in the reference paper was the modified Shepp-Logan image and the justification for parameters chosen in this project was based on it, there is possibility that GFFT performs much better than LS_NUFFT. For further correction, therefore, parameters should be determined through careful optimization procedures instead of simply using ones provided in the reference. However, we can still claim that this LS_NUFFT technique has consistent superiority to Kaiser-Bessel model. In subsequent section different version of LS_NUFFT was developed by using Gaussian scale factor other than cosine one. Kernel function and several resultant images were calculated based on that.

Additional comparison of LS_NUFFT with Gaussian NUFFT

In the final section, the analytic kernel formulation for Gaussian scaling factor[3] was defined as follows.

$$
\begin{aligned}
&\rho_{j,cp} = G_{j,k} a_{k,cp} \\
&G = F^{-1}, F_{j,k} = \frac{-2i\sin(\pi(j-k)/m)}{1-\exp(i2\pi(j-k)/mN)} \\
&a_{k,cp} = \sum_{n=-N/2}^{N/2-1} \exp\left(-b\left(\frac{2\pi n}{Nm}\right)^2 + i\frac{2\pi n}{Nm}\left(\{mc_p\}+k\right)\right) \\
&\{mc_p\} = mc_p - [mc_p] \\
&j,k = -\frac{q}{2}\cdots\frac{q}{2} \\
&p = 1,\ldots M
\end{aligned}
\qquad \text{Eq.(5)}
$$

Since in LS_NUFFT the kernel matrix is strongly linked to the scaling factor through optimization, it is essential to carefully derive kernel values based on different types of scaling functions. In previous case, cosine function was used as a scaling factor. The difference can be seen for $a_{k,cp}$ term in Eq.(5) compared to Eq.(4). Another thing to mention is that G matrix in Eq.(5) is independent of no matter what scaling factor is used,

while $a_{k,cp}$ is still dependent on it. After taking into consideration all those points made, reconstructed images were obtained with different values of b. b parameter plays certain role in standard deviation of Gaussian function which is inversely proportional to it. Therefore, it can be easily expected that better image will be reconstructed with larger b. Resultant images confirm that point as shown in Fig.11, 12, 13, and 14. Distance measure D was also calculated and given in Table 4.

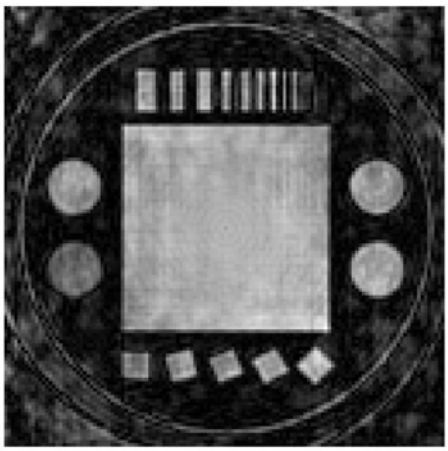

Fig.11. Reconstructed image using Gaussian NUFFT with b=0.1

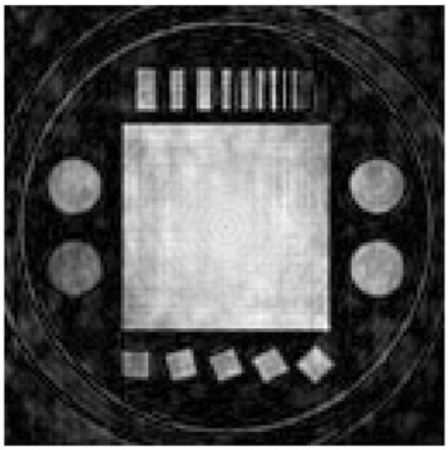

Fig.12. Reconstructed image using Gaussian NUFFT with b=0.5

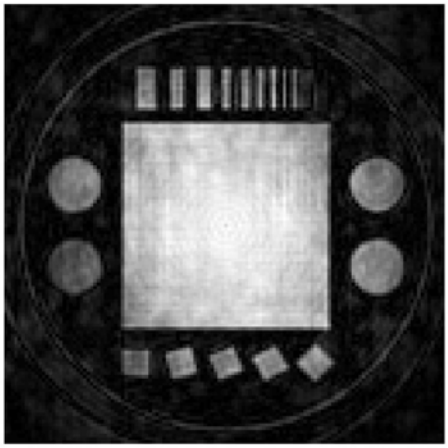

Fig.13. Reconstructed image using Gaussian NUFFT with b=1

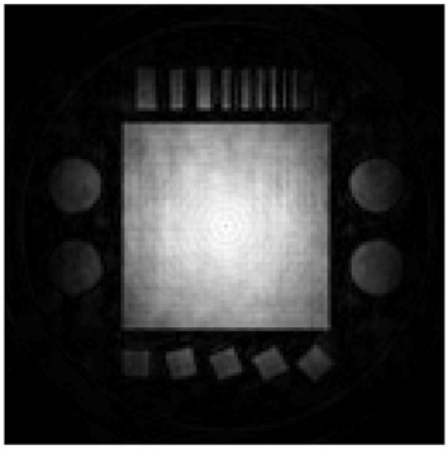

Fig.14. Reconstructed image using Gaussian NUFFT with b=3

Table 4. Distance measures for Gaussian NUFFT with different b values

b parameter	Distance measure($Dx10^{-2}$)
b=0.1	7.73
b=0.5	6.66
b=1	5.92
b=3	4.31

In Table 4 problems rise when b value goes higher than 1. As Gaussian function gets narrower, higher frequency terms are much suppressed. Although distance measure decreases towards higher values of b, image contrast is significantly degraded. Therefore, compromise between distance measure and image contrast should be taken great care of

when Gaussian scale factor is being used. As a result, with given phantom image, LS_NUFFT with cosine scale factor has much better performance than that of Gaussian NUFFT. The reason for this result is also explained in a way that cosine function originates from sampled triangle kernel which has less ripples compared to Gaussian case.

Reference

[1] Liewei Sha, " An Improved Gridding Method for Spiral MRI Using Non-uniform Fast Fourier Transform", J.Magn.Reson.(162), pp.250-258, 2003

[2] Nhu Nguyen and Qing huo Liu, "The Regular Fourier Matrices and Non-uniform Fast Fourier Transforms", SIAM J.SCI.COMPUT. Vol.21(1), pp.283-293, 1999

[3] J. O'Sullivan, "A Fast Sinc Function Gridding Algorithm for Fourier Inversion in Computer Tomography", IEEE Trans.Med.Imaging 4(MI-4), pp.200-207, 1985

[4] G.Sarty, " Direct Reconstruction of Non-Cartesian k-Space Data Using A Non-uniform Fast Fourier Transform", Magn.Reson.Med.(45), pp.908-915, 2001